Correlated evolution of structure and mechanical loss of a sputtered silica film

Massimo Granata,[1,*] Elodie Coillet,[2] Valérie Martinez,[2,†] Vincent Dolique,[1] Alex Amato,[1] Maurizio Canepa,[3,4] Jérémie Margueritat,[2] Christine Martinet,[2] Alain Mermet,[2] Christophe Michel,[1] Laurent Pinard,[1] Benoît Sassolas,[1] and Gianpietro Cagnoli[1,2]

[1]*Laboratoire des Matériaux Avancés, CNRS/IN2P3, F-69622 Villeurbanne, France*

[2]*Institut Lumière Matière, CNRS (UMR 5306), Université de Lyon, F-69622 Villeurbanne, France*

[3]*OPTMATLAB, Dipartimento di Fisica, Università di Genova, Via Dodecaneso 33, 16146 Genova, Italy*

[4]*INFN, Sezione di Genova, Via Dodecaneso 33, 16146 Genova, Italy*

(Received 14 June 2017; published 21 May 2018)

Energy dissipation in amorphous coatings severely affects high-precision optical and quantum transducers. In order to isolate the source of coating loss, we performed an extensive study of Raman scattering and mechanical loss of a thermally treated sputtered silica coating. Our results show that loss is correlated with the population of three-membered rings of Si-O_4 tetrahedral units and support the evidence that thermal treatment reduces the density of metastable states separated by a characteristic energy of about 0.5 eV in favor of an increase of the density of states separated by smaller activation energies.

DOI: 10.1103/PhysRevMaterials.2.053607

I. INTRODUCTION

Thermal noise in amorphous dielectric materials is a fundamental limitation for a large number of precision experiments based on optical and quantum transducers, such as gravitational-wave detectors [1], optomechanical resonators [2], frequency standards [3], quantum computers [4], and atomic clocks [5]. In these devices, thermally driven random structural relaxations introduce decoherence in vibrational or electronic states. Any observable that is related to these states experiences fluctuations, i.e., noise. In mechanical experiments, this decoherence distributes the thermal energy of vibrations, stored in the normal modes, all over the frequency spectrum.

As stated by the fluctuation-dissipation theorem [6], the same structural relaxations give origin to energy dissipation: In linear systems at the thermodynamic equilibrium, the power spectral density of the fluctuations associated to any observable is proportional to the dissipative part of their dynamics. This fact is of the utmost importance, since in many cases the fluctuations are difficult to measure, whereas the energy dissipation is in general more accessible. Dissipation of mechanical energy in materials is quantified by the so-called loss angle $\phi = \tan^{-1}(\Im(E)/\Re(E))$, where $\Im(E)$ and $\Re(E)$ are the imaginary and real part of the Young's modulus E, respectively. Although in principle there should be a loss angle associated to each elastic constant, we assume here that ϕ is the same for all of them; our measurements confirm this hypothesis. In the harmonic analysis, the imaginary part of the elastic constant is related to the retarded response of the material (anelasticity) [7].

In amorphous materials, the loss comes from unknown relaxation processes whose features are fairly well explained by the asymmetric double-well potential model [8]: The structure changes locally between two metastable states separated by a barrier of height V and has a typical relaxation time $\tau \propto e^{V/k_BT}$. As a consequence, loss is a function of temperature, $\phi \equiv \phi(T)$. Remarkably, the temperature dependence is similar in many different bulk amorphous materials [9], suggesting that this property might be determined by a set of universal laws. In amorphous coatings, on the contrary, the structure as well as $\phi(T)$ vary with the synthesis process.

Within this landscape, silica (SiO_2) shows an unusual and extremely interesting behavior, which makes it a suitable candidate to study the relaxation mechanisms of structural loss. In its bulk form, i.e., fused silica, the internal friction $\phi \sim 5 \times 10^{-9}$ is about 4 orders of magnitude lower than any other metal oxides at $T_0 \sim 300$ K [9,10]; yet, if deposited as a ion-beam sputtered (IBS) film, it shows a much higher damping—$\phi \sim 2{-}5 \times 10^{-5}$ at T_0 [11–13]. A change in the energy distribution of relaxation mechanisms is likely responsible of this behavior, but, despite the fact that silica is one of the most studied glass in material science and that its $\phi(T)$ is nowadays very well characterized [14–16], these mechanisms are still unknown. In order to isolate such mechanisms, we performed an extensive study of Raman scattering and loss of a thermally treated IBS silica coating, and we addressed the possible correlations between damping and structure. The structure of silica is a three-dimensional network composed of SiO_4 tetrahedral units arranged in rings of assorted sizes, from 3 to 10 tetrahedra [17]. Raman spectroscopy is sensitive to the vibration of local structures in vitreous systems at short- to middle-range scale (few to 10 Å) and particularly to the distribution of angles between tetrahedra and to the population of threefold and fourfold rings.

II. EXPERIMENT

We deposited the silica coating on a fused silica disk-shaped mechanical resonator (∅ 3″, 1 mm thick) for the characterization of loss and on a fused silica tablet (∅ 1″, 5 mm

*m.granata@lma.in2p3.fr

†valerie.martinez@univ-lyon1.fr

thick) for the Raman study. Prior to deposition, the disk was annealed at 900 °C for 10 h and the tablet has been coated with 100 nm of tantalum (which has no active Raman vibrational modes) in order to acquire the signal of the silica coating only.

Amorphous SiO_2 coating (3 μm) has been deposited on both sides of the disk and on the metal-coated surface of the tablet, in a Veeco SPECTOR dual-IBS chamber. Argon and oxygen were fed into both sources, with flow rates of 18 sccm and 15 sccm in the sputtering source and 3 sccm and 12 sccm in the assistance source, respectively. During the coating process, the energy of the coating particles impinging on the substrate was of the order of 10 eV, and the temperature of the substrates was approximately 80 °C. After coating, both samples have been repeatedly annealed together at 500 °C, a temperature much lower than the silica glass-transition temperature $T_g \sim 1200$ °C, for progressively increasing time. A typical annealing temperature for optical coatings is 500 °C [12,18]. The Raman spectrum and the coating loss have been measured at room temperature after each annealing step to follow at the same time the evolution of structure and damping.

Raman spectra were recorded with a LabRAM HR Evolution micro-Raman spectrometer, equipped with three super-notch filters to attenuate the Rayleigh line and with a Peltier-cooled charge-coupled device. The incident light was emitted by a YAG:Nd^{3+} laser at 532 nm. Spectra were recorded from 200 to 900 cm^{-1} with a ×100 objective delivering 6 mW on the sample, avoiding heating or sample damage. To measure the coating loss, we applied the resonance method [7] to the disk, measuring the ring-down time τ of eight vibrational modes from 1 to 17 kHz. For each mode of frequency f_n, the loss $\phi_n = \pi f_n \tau_n$ is the linear combination of the losses of substrate and coating, where the coefficients are the fraction of elastic energy stored in each part. The double measurement of loss before and after the coating deposition allows the estimation of the coating loss only [12]. A clamping-free system named Gentle Nodal Suspension [19] has been used to suspend the disk, as it highly suppresses the systematic damping due to suspension and allows a high reproducibility of the results [20]. More details about our experimental setup can be found elsewhere [12].

III. RESULTS

Figure 1(a) shows that some spectroscopic features of our film are similar to those of densified silica. The density ρ of our film can be inferred from its correlation with the half width at half maximum of the main band ($HWHM_{MB}$), established for fused silica samples that underwent a cycle of densifications obtained after a hydrostatic high-pressure cycle (up to 26 GPa and 2.66 g/cm^3) at room temperature [21]. Using this curve and measuring $HWHM_{MB}$ for our sputtered silica [Fig. 2(a)], we obtain $\rho = 2.37 \pm 0.02$ g/cm^3. This is in agreement with the independent estimate $\rho = 2.33 \pm 0.04$ g/cm^3, obtained through the direct measurement of coating mass with an analytical balance and through the analysis of spectroscopic-ellipsometry measurements with a J. A. Woollam VASE instrument, yielding coating thickness and refraction index. The densification can be inferred also from the frequency ω_{MB} of the main band maximum, which corresponds mainly to the bending mode of bridging oxygen (Si-O-Si). ω_{MB} is directly linked to the mean intertetrahedral angle θ via the Sen and

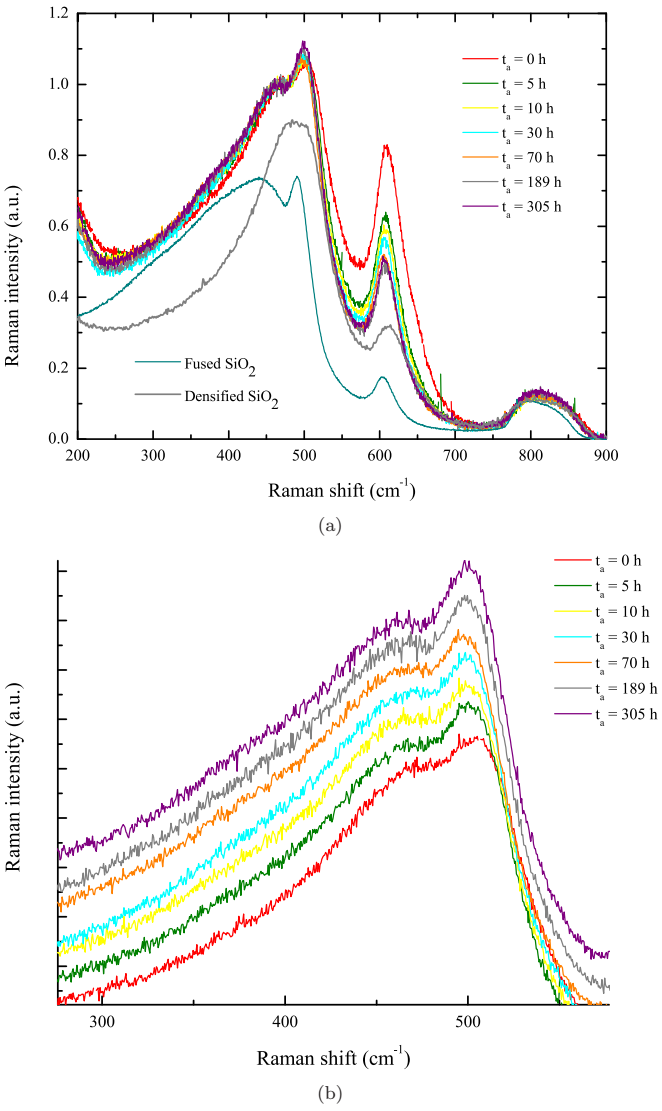

FIG. 1. Raman spectra of SiO_2: (a) Comparison of the as-deposited coating ($t_a = 0$ h) to fused silica, densified silica, and thermally treated coating with different cumulative annealing time t_a. Coating spectra have been normalized to the amplitude of the main band; the spectra of fused silica and densified silica have been arbitrarily shifted along the ordinate axis for clarity; (b) zoom on peak positions of main and D_1 bands of as-deposited ($t_a = 0$ h) and thermally treated coating. Spectra have been arbitrarily shifted along the ordinate axis for clarity.

Thorpe central-force model [22],

$$\omega_{MB} = \left(2\frac{\alpha}{m_O}\right)^{\frac{1}{2}} \cos\left(\frac{\theta}{2}\right), \quad (1)$$

where $\alpha = 1.622 \times 10^{-7}$ $g/mol/cm^2$ is the restoring constant central force between Si and O atoms and $m_O = 16$ g/mol is the oxygen mass. For fused silica, $\theta \sim 144°$, corresponding to $\omega_{MB} = 435 \pm 1$ cm^{-1}, and this value decreases with the densification ratio $\Delta\rho/\rho$ [21]. For our coating $\omega_{MB} = 477 \pm 1$ cm^{-1}, and thus $\theta \sim 141°$.

In fused silica, the ring statistic—characteristic of medium range order of silicate glasses—is peaked on sixfold rings

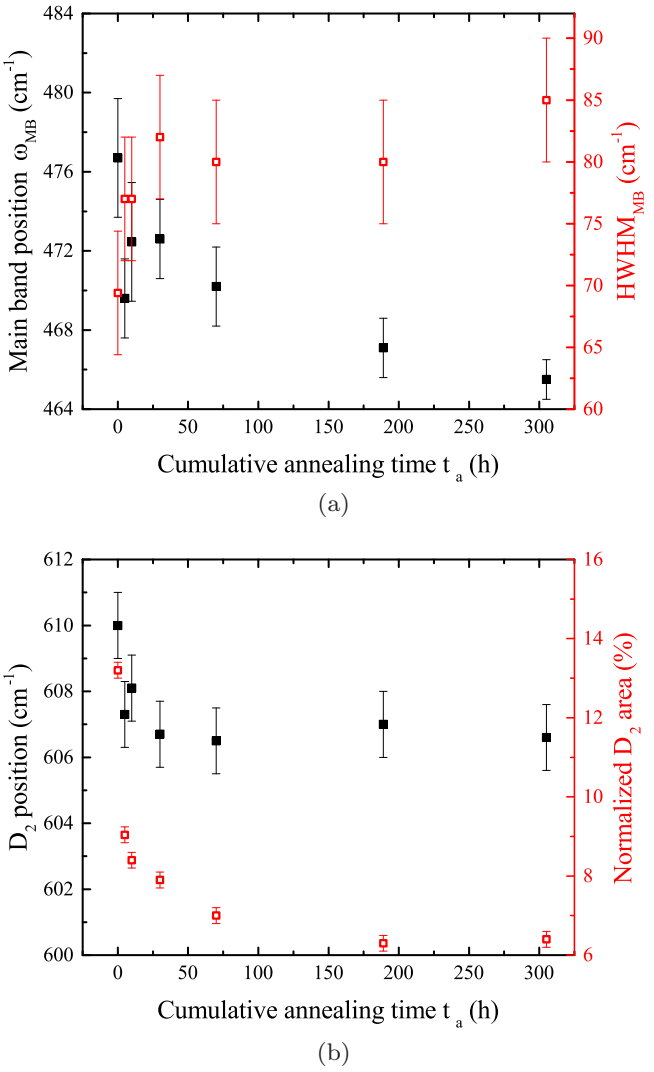

FIG. 2. Evolution of the film spectral features as a function of the cumulative annealing time t_a: (a) ω_{MB} and $HWHM_{MB}$ and (b) D_2 area (normalized to the area of the spectrum from 230 to 700 cm^{-1}) and position.

[17,23] and is shifted towards smaller rings when density increases via cold compression [17] beyond the elastic limit. The two sharp bands at 490 cm^{-1} (hereafter D_1) and at 605 cm^{-1} (D_2) are assigned to fourfold and threefold ring breathing modes, respectively, and it has been shown [24,25] that the normalized D_2 area is related to the threefold ring population. From Fig. 1(a), we observe that in the coating spectrum both D_1 and D_2 are more intense than in the spectra of both fused silica and densified silica. Its D_2 area (normalized to the area from 230 to 700 cm^{-1}) is higher than that of both densified and fused silica (of about 6 times compared to the latter). Finally, the D_2 position in our film is shifted towards higher frequencies with respect to that of fused silica [Fig. 2(b)]: This finding indicates the presence of an internal stress. Following Ref. [26], the D_2 shift of 5 cm^{-1} corresponds to a 0.4 ° decrease of the Si-O-Si angles due to stress-induced ring puckering [27,28].

Figures 1(a) and 1(b) show the Raman spectra of the annealed coating for different cumulative annealing time t_a, increasing from 5 to 300 h, compared to the as-deposited (t_a = 0 h) coating spectrum. The evolution of the coating spectral features as a function of t_a is shown in Figs. 2(a) and 2(b). ω_{MB} shifts from 477 ± 1 cm^{-1} at $t_a = 0$ h to 466 ± 1 cm^{-1} at $t_a = 300$ h, without reaching a plateau. This corresponds to an increase $\Delta\theta = 0.9°$, which is coherent with Fourier-Transform infrared spectroscopy measurements of sputtered silica coatings showing that θ increases with annealing [29] and can be related to a less dense structure. $HWHM_{MB}$ increases along with t_a, denoting a widening of the θ distribution: $HWHM_{MB}$ is 69 ± 5 cm^{-1} at $t_a = 0$ and 85 ± 5 cm^{-1} at $t_a = 300$ h. For comparison, $HWHM_{MB} \sim 120 \pm 10$ cm^{-1} for fused silica. Thus the annealed film is less homogeneous in terms of θ values than the as-deposited film.

The normalized D_2 area decreases monotonically, following a stretched exponential law [29] with $\tau = 6.3 \pm 1.1$ h and $\beta = 0.36 \pm 0.05$. This relaxation time is relatively short: magnetron-sputtered silica deposited at 520 °C has the same relaxation time at about 800 °C, and follows the Arrhenius law with activation energy of 5.4 ± 0.2 eV [29]. Considering also that relaxation times of fused silica (with fictive temperature $T_f = 1100$ °C) are 6×10^4 times longer [29], we might say that the deposition temperature is more effective than the annealing temperature in stabilizing sputtered silica. Unfortunately, those data are not conclusive since relaxations in Ref. [29] were observed in the infrared reflectivity (stretching mode of Si-O-Si), whereas our data concern the D_2 evolution, and the fact that in Ref. [29] $\beta < 0.3$ indicates the presence of a broad spectrum of relaxation mechanisms.

It is more difficult to quantify the evolution of the fourfold ring population, since the D_1 band is partly overlapping with the main band and their deconvolution is not trivial. Qualitatively, D_1 population increases with t_a.

All the above measurements lead to explain the structural evolution of our silica coating by stress relaxation. It is worth clarifying that such stress is internal and cannot be removed if the film is detached from the substrate. We propose here that the internal stress accelerates the relaxations. This can justify why our low-temperature-deposited silica relaxes faster than a high-temperature-deposited one and still faster than fused silica [29] (we can assume that this latter is free of stress). Our IBS silica reached a plateau, but this does not correspond to a stress-free structure.

Our loss measurements are shown on Fig. 3(a), where each data series corresponds to a given value of t_a. The heat treatment progressively reduces the loss, the most dramatic decrease happening for $t_a = 5$ h. For the outliers at 10.5 and 14.6 kHz, the estimated coating energy fraction is different from the computed one; as this is not explained so far, we excluded them from the computation of the frequency-averaged coating loss $\langle\phi\rangle_\omega$ presented in Fig. 3(b) (as they would only induce an offset which would not change our analysis). The observed loss evolution is due to the coating only: The substrate being annealed at 900 °C before deposition, no variation of loss has been measured after the postdeposition annealing at 500 °.

The correlation between the normalized D_2 area and $\langle\phi\rangle_\omega$ is shown in Fig. 4. Clearly, $\langle\phi\rangle_\omega$ increases monotonically with the area underlying the D_2 line, and thus with the threefold ring population. Figure 4 also shows a data point relative to another

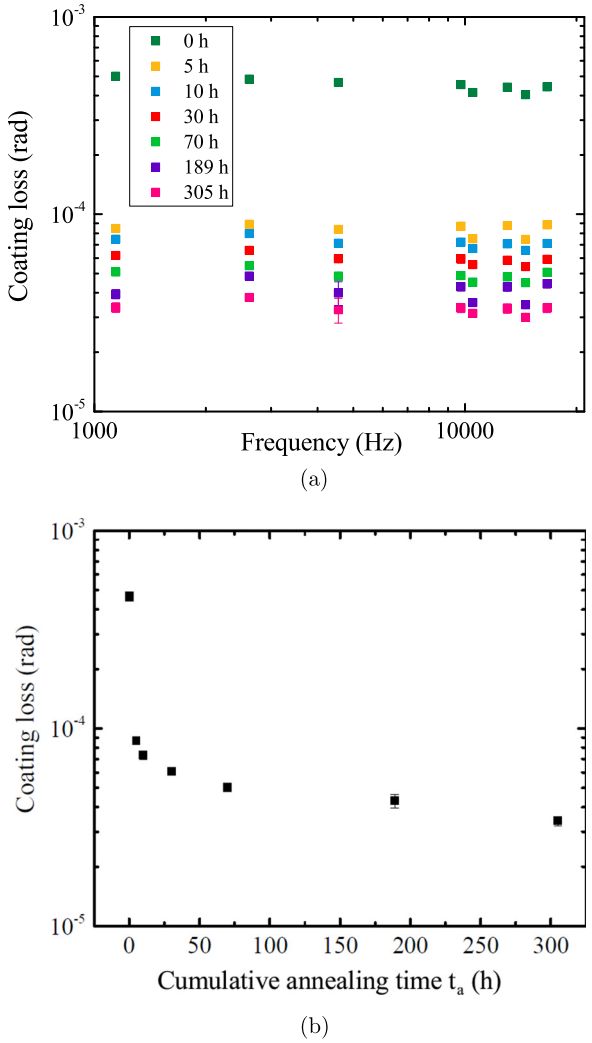

FIG. 3. Results of the mechanical characterization: (a) coating loss as a function of frequency, for different values of the cumulative annealing time t_a; (b) frequency-averaged coating loss $\langle\phi\rangle_\omega$ as a function of t_a.

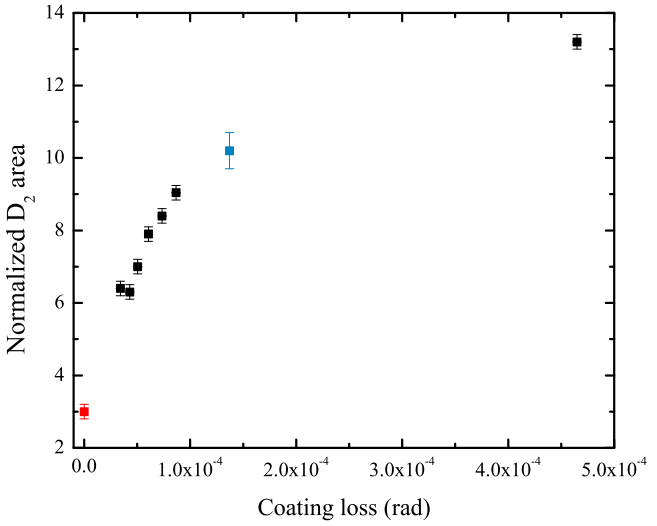

FIG. 4. Correlation between D_2 area (normalized to the area of the spectrum from 230 to 700 cm^{-1}) and frequency-averaged loss $\langle\phi\rangle_\omega$, for silica films deposited in the SPECTOR (black) and in the Grand Coater (light blue) and for fused silica (red).

IBS silica film (not annealed) that we deposited with a different set of parameters [12,13] in the large custom-developed *Grand Coater* used to deposit the Bragg reflectors on the mirrors of all present ground-based gravitational-wave interferometers and a data point that we measured on fused silica as well: The correlation still holds. Recent molecular-dynamics simulations [30] established that structural relaxation comes from the twisting of chains of few tens of SiO_4 tetrahedra, via rotation and stretching of Si-O bonds; between 10 and 10^2 atoms are involved in this reorganization, but an investigation on the ring population inside these relaxing chains has not yet been carried out at present.

Relaxation mechanisms active at room temperature and at acoustic frequencies should have barrier heights of about 0.5 eV [8]. The activation energy of three-membered rings has been measured to be about 0.43 eV [28,31]. The similarity between these energies could explain why loss and D_2 ring population are correlated: The annealing reduces the density of metastable states separated by about 0.5 eV, in favor of an increase of the density of states separated by smaller activation energies. This increase is suggested by our measurements, as shown by the increase of the D_1 ring population and by low-temperature ($T < 100$ K) loss measurements [32]. These latter measurements show that densified silica has less internal friction than fused silica at 12 kHz. Fused silica shows a loss peak at 30 K compatible with a distribution of barrier heights centered around 50 meV.

It is not clear whether the metastable states related to the threefold rings are involved in the relaxations that cause the loss in IBS silica coatings. The relaxation time of our IBS silica, as measured from the loss data, is 5 ± 2 min ($\beta = 0.18 \pm 0.02$); loss in fused silica is several orders of magnitude lower than in our coating, despite the amplitude of its D_2 line [Fig. 1(a)]. These facts suggest that metastable structures relevant for loss are different from threefold rings.

IV. CONCLUSIONS

In summary, IBS deposition leads to a dense and internally stressed silica film. This outcome is consistent with previous studies showing that IBS and ion-assisted deposition yield highly densified silica coatings [29,32–35]. Thanks to internal stress, IBS silica relaxes towards a less dense structure even if $T \ll T_g$. The loss of the silica coating is correlated with the population of threefold rings, and this correlation holds even when the coating structure is determined by different deposition parameters. Threefold rings could be involved in the relaxation mechanisms if included in more complex structures; further molecular-dynamics simulations could elucidate this point through a dedicated study of ring statistics.

ACKNOWLEDGMENTS

The authors gratefully acknowledge support from the LabEx Lyon Institute of Origins (LIO, Grant No. ANR-10-

LABX-0066) within the program "Investissements d'Avenir" (Grant No. ANR-11-IDEX-0007) of the French National Research Agency (ANR) and thank the CECOMO Platform of vibrational spectroscopy.

[1] R. X. Adhikari, Rev. Mod. Phys. **86**, 121 (2014).
[2] M. Aspelmeyer *et al.*, Rev. Mod. Phys. **86**, 1391 (2014).
[3] T. Kessler *et al.*, Nat. Photon. **6**, 687 (2012).
[4] J. M. Martinis, K. B. Cooper, R. McDermott, M. Steffen, M. Ansmann, K. D. Osborn, K. Cicak, S. Oh, D. P. Pappas, R. W. Simmonds, and C. C. Yu, Phys. Rev. Lett. **95**, 210503 (2005).
[5] A. D. Ludlow *et al.*, Rev. Mod. Phys. **87**, 637 (2015).
[6] H. B. Callen and R. F. Greene, Phys. Rev. **86**, 702 (1952).
[7] A. Nowick and B. Berry, *Anelastic Relaxation in Crystalline Solids* (Academic Press, New York, 1972), pp. 582–602.
[8] K. S. Gilroy and W. A. Phillips, Philos. Mag. B **43**, 735 (1981).
[9] K. A. Topp and D. G. Cahill, Z. Phys. B **101**, 235 (1996).
[10] A. Ageev *et al.*, Class. Quantum Grav. **21**, 3887 (2004).
[11] M. Principe, I. M. Pinto, V. Pierro, R. DeSalvo, I. Taurasi, A. E. Villar, E. D. Black, K. G. Libbrecht, C. Michel, N. Morgado, and L. Pinard, Phys. Rev. D **91**, 022005 (2015).
[12] M. Granata, E. Saracco, N. Morgado, A. Cajgfinger, G. Cagnoli, J. Degallaix, V. Dolique, D. Forest, J. Franc, C. Michel, L. Pinard, and R. Flaminio, Phys. Rev. D **93**, 012007 (2016).
[13] A. Amato *et al.*, J. Phys. Conf. Ser. **957**, 012006 (2018).
[14] S. D. Penn *et al.*, Phys. Lett. A **352**, 3 (2006).
[15] F. Travasso *et al.*, Europhys. Lett. **80**, 50008 (2007).
[16] I. W. Martin *et al.*, Class. Quant. Grav. **31**, 035019 (2014).
[17] W. Jin, R. K. Kalia, P. Vashishta, and J. P. Rino, Phys. Rev. B **50**, 118 (1994).
[18] L. Anghinolfi *et al.*, J. Phys. D: Appl. Phys. **46**, 455301 (2013).
[19] E. Cesarini *et al.*, Rev. Sci. Instrum. **80**, 053904 (2009).
[20] M. Granata *et al.*, Arch. Metall. Mater. **60**, 365 (2015).
[21] C. Martinet *et al.*, J. Phys.: Condens. Matter **27**, 325401 (2015).
[22] P. N. Sen and M. F. Thorpe, Phys. Rev. B **15**, 4030 (1977).
[23] L. Huang and J. Kieffer, Phys. Rev. B **69**, 224204 (2004).
[24] A. Pasquarello and R. Car, Phys. Rev. Lett. **80**, 5145 (1998).
[25] J. Burgin, C. Guillon, P. Langot, F. Vallée, B. Hehlen, and M. Foret, Phys. Rev. B **78**, 184203 (2008).
[26] B. Hehlen, J. Phys.: Condens. Matter **22**, 025401 (2009).
[27] C. J. Brinker *et al.*, J. Non-Cryst. Solids **99**, 418 (1988).
[28] R. A. Barrio, F. L. Galeener, E. Martínez, and R. J. Elliott, Phys. Rev. B **48**, 15672 (1993).
[29] T. Hirose *et al.*, J. Non-Cryst. Solids **352**, 2198 (2006).
[30] R. Hamdan *et al.*, J. Chem. Phys. **141**, 054501 (2014).
[31] N. Shimodaira, K. Saito, E. H. Sekiya, and A. J. Ikushima, Phys. Rev. B **73**, 214206 (2006).
[32] G. Weiss *et al.*, Physica B (Amsterdam) **219-220**, 290 (1996).
[33] P. J. Martin *et al.*, Appl. Opt. **22**, 178 (1983).
[34] W. G. Sainty *et al.*, Appl. Opt. **23**, 1116 (1984).
[35] B. S. Bhumbra *et al.*, J. Vac. Sci. Technol. B **13**, 881 (1995).